


SCIENTIFIC REPORTS



OPEN

Development of a numerical model to predict physiological strain of firefighter in fire hazard

Yun Su^{1,2}, Jie Yang², Guowen Song², Rui Li², Chunhui Xiang²  & Jun Li^{1,3}

This paper aims to develop a numerical model to predict heat stress of firefighter under low-level thermal radiation. The model integrated a modified multi-layer clothing model with a human thermoregulation model. We took the coupled radiative and conductive heat transfer in the clothing, the size-dependent heat transfer in the air gaps, and the controlling active and controlled passive thermal regulation in human body into consideration. The predicted core temperature and mean skin temperature from the model showed a good agreement with the experimental results. Parametric study was conducted and the result demonstrated that the radiative intensity had a significant influence on the physiological heat strain. The existence of air gap showed positive effect on the physiological heat strain when air gap size is small. However, when the size of air gap exceeds 6 mm, a different trend was observed due to the occurrence of natural convection. Additionally, the time length for the existence of the physiological heat strain was greater than the existence of the skin burn under various heat exposures. The findings obtained in this study provide a better understanding of the physiological strain of firefighter and shed light on textile material engineering for achieving higher protective performance.

Skin burn is one of the most common thermal injuries in firefighting and emergency rescue. Heat stroke of life-threatening injury also usually occurs during the firefighting task. According to recent statistics of firefighter fatalities in the United States, 40 out of 68 deaths in 2015 resulted from heat stress or overexertion that led to heart attack or stroke¹. Almost two-thirds of the firefighters over age 40 who died in 2015 was due to heart attacks or other cardiac events¹. The level of physiological strain developed during the firefighting has an important effect on the physical capability, cognitive function, work tolerance, and even physical injuries and illness (e.g., heat stroke)^{2,3}.

In the past, most studies in intensive radiation and flash fire focused on the skin burn injury. Thermal Protective Performance (TPP) tester was developed to evaluate thermal protective performance of fabric under a combination of radiant and convective heat exposure⁴. Radiative protective performance of fabric under high-level thermal radiation could be examined by using Radiant Protective Performance (RPP) tester⁵. The protective performance of fabric under low-level thermal radiation was evaluated based on a stored thermal energy tester regulated by ASTM F2731-11⁶. The results demonstrated that the skin burn injury depended not only on the type and intensity of heat source⁷, but also on the fabric's category and configuration⁸, the air gap size^{9,10} and the fit and design features of clothing^{11,12}.

However, prevention of the skin burn injury does not guarantee the definite security for firefighters, since the heat stroke can occur under no skin burn. The skin burn injury is generally induced by thermal radiation or heat source, while the human physiological strain associated with firefighting is caused by a combined effect of thermal environments (e.g. fires and radiation) and strenuous work¹³. As a result, firefighting protective clothing has different effects on the skin burn and the human physiological strain. The protective clothing can provide a positive effect on preventing the skin burn and the physiological strain by resisting heat transfer from thermal environment to human body. However, the protective clothing also increases the burden of wearers due to its heavy and low permeability characteristics, especially in hot environments^{2,14}. Therefore, protective measures which aim at avoiding skin burn does not necessarily reduce the human physiological strain. Accordingly, there is an urgent

¹College of Fashion and Design, Donghua University, Shanghai, 200051, China. ²Iowa State University, Ames, 50010, Iowa, USA. ³Key Laboratory of Clothing Design and Technology, Donghua University, Ministry of Education, Shanghai, 200051, China. Correspondence and requests for materials should be addressed to G.S. (email: gwsong@iastate.edu)

need to develop a further understanding of the physiological responses of firefighter in thermal environment and take measures to reduce the heat strain.

The physiological strain of firefighter can be investigated based on human trials in a simulated operating state of firefighter. The physiological reaction, such as heart rate, oxygen consumption, blood lactate concentration, skin temperature and core temperature, were measured to assess the human physiological strain in thermal environment¹⁵. For example, Hemmatjo *et al.*¹⁶ assessed the effect of various hot environments (low heat, moderate heat and severe heat) on the firefighters' physiological responses. The lab and field trials were performed by Annaheim *et al.*¹⁷ to examine the effect of environmental heat and physical activity on thermo-physiological responses. Fontana *et al.*¹⁸ investigated the effect of different fabric layers of protective clothing on thermo-physiological responses of human study participants. Considering the safety and well-being of the trial subjects, however, the human physiological strain was only examined in the absence of environmental heat or in relatively low intensity heat environments that are not enough to simulate the risk of heat stroke of firefighter in common fire scenes. Therefore, it is extremely important to develop a safe evaluation method for investigating the human physiological strain of firefighter in a simulated fire environment.

With the rapid development of computer technology, numerical simulation has been widely used to simulate heat transfer in clothing and predict body physiological strain in recent decades. Comparing to the laboratory simulation method, the numerical simulation method can remedy the experimental limitation, by studying the physiological reaction of firefighter under simulated fire environments, such as flash fire and thermal radiation. In previous applications, numerical models of heat transfer in firefighting protective clothing subjected to different fire hazards have been developed^{19–22}. In the early 1970s, Morse *et al.*¹⁹ modeled the thermal response of protective clothing subjected to a JP-4 fuel fire that considered the effect of pyrolysis, ignition, and combustion of fabric. One of the most significant developments on heat transfer in firefighting protective clothing was the introduction of Torvi's model²⁰. This numerical model proved that one-dimensional model effectively simulated heat transfer in firefighting protective clothing. A clothing numerical model developed by Song *et al.*²¹ was employed to explain heat transfer in a configuration that realistically simulates the shape of human body. The model considered simulated fire nature, temperature dependent fabric properties and air gaps distribution²¹. In regard to the heat transfer in low-level thermal radiation, several efforts were made on model development. A multi-layer fabric model in low-level thermal radiation was developed to simulate the transmitted and stored thermal energy within protective clothing²².

However, these developed models only focused on heat transfer on human skin burn injury, and are generally coupled with skin bio-heat transfer and burn models for predicting skin burn injuries in fire hazards. The model of skin burn prediction simplified body thermal regulation and did not predict the human physiological reaction to thermal environment²³. Considering the effect of heat stress on operation safety of firefighter¹, the physiological strain can be a more critical index to determine the health and safety of firefighter than the skin burn. Thus, it is significant to develop a numerical model on heat transfer in firefighting protective clothing which is coupled with human thermal regulation for investigating the human physiological reaction in fire hazards. In addition, the fire hazards confronted by firefighter are usually divided into three categories: routine, hazardous and emergency²⁴. Since statistics showed that most of firefighting assignments are performed under routine condition (low-level thermal radiation) for a relatively prolonged periods of time²⁵, it is more reasonable to firstly consider the low-level thermal radiation.

Therefore, the objective of this study is to predict physiological thermal strain of firefighter in low-level thermal radiation while simultaneously monitoring the skin burn injury. A heat transfer model is developed that describes heat transfer from radiative thermal environment to human body through multilayer protective clothing. The model is coupled with an improved human thermal regulation effects. The developed model is used to evaluate the effect of thermal environment and clothing on the physiological thermal strain developed to firefighters during exposure.

Mathematical model

Firefighting protective clothing consists of outer shell, moisture barrier and thermal liner. In this work, a multilayer protective clothing system with air gaps of various sizes is focused. A radiant thermal environment is simulated with a nominal heat flux of 8.5 kW/m², as is shown in Fig. 1¹⁶. A multi-node thermal regulation model is developed to simulate heat transfer in human body. The model incorporates the human body into four-layer structure including skin, fat, muscle and core. A human body is divided as 20 body parts according to body physiological characteristics and the 20-zone manikin 'Newton' (Thermetrics, Seattle, USA)²⁶. Model assumptions are given as below to simplify the formulation:

- (1) Thermal energy from heat source to outer shell is transmitted in radiant mode. The radiative and convective heat loss between clothing and the surrounding environment is considered.
- (2) The clothing model is one-dimensional heat transfer model along the thickness direction of the clothing layers.
- (3) The radiative and conductive heat transfer is coupled in the clothing model; while the effect of convective heat transfer within the clothing layer is neglected²¹.
- (4) The thermal properties of the clothing layers are taken to be a function of temperature, but the optical properties of the clothing layers, such as absorptivity, reflectivity and transmissivity, are assumed as constant values.
- (5) The radiative and conductive heat transfer in the air gap between thermal liner and skin surface is considered. The occurrence of convective heat transfer depends on the air gaps size and temperature difference between the thermal liner and the skin surface.
- (6) Initial conditions are uniform throughout the clothing layer and the air gaps.

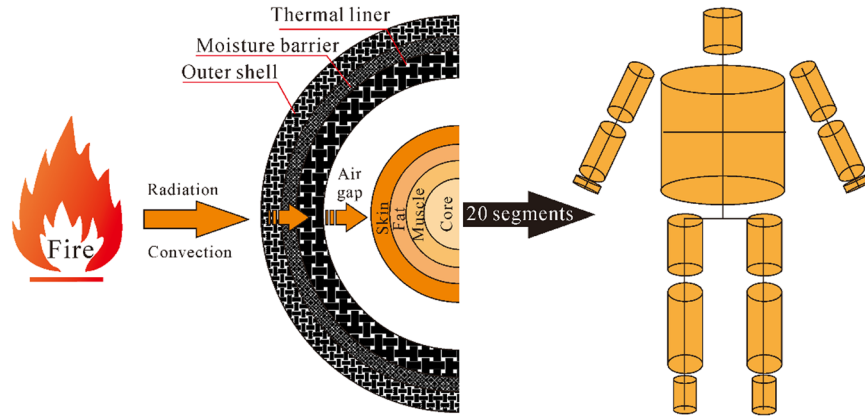


Figure 1. Schematic of heat transfer in “thermal environment– clothing– air gap– human body” system.

- (7) 20 segments of human body are exposed to the thermal radiation of same intensity.
- (8) The effects of evaporation heat loss from skin sweats, the increased blood flow rate due to high temperature condition, and the vasodilatation on the body heat transfer are simulated.

Heat transfer in clothing layers. Heat exchange on the surface of the outer shell includes the radiant heat transfer from heat source, and the coupled convection and radiation between the outer shell and the surrounding environment. For cooling phase, there is no radiant heat transfer from the heat source. The heat exchange equations during the heat exposure and cooling phases are written as, respectively:

$$-k_1 \frac{\partial T}{\partial x} \Big|_{x=0} = -h_{conv,amb1}(T|_{x=0} - T_{amb}) - \sigma \varepsilon_1 F_{shell-amb}(1 - \varepsilon_g)(T^4|_{x=0} - T_{amb}^4) \quad 0 < t < t_{exp} \quad (1)$$

$$-k_1 \frac{\partial T}{\partial x} \Big|_{x=0} = -h_{conv,amb2}(T|_{x=0} - T_{amb}) - \sigma \varepsilon_1(T^4|_{x=0} - T_{amb}^4) \quad t > t_{exp} \quad (2)$$

where k_1 is the outer shell thermal conductivity; $h_{conv,amb1}$ and $h_{conv,amb2}$ are the convective heat transfer coefficient between the outer shell and the ambient during the exposure and the cool down phase, respectively; $T|_{x=0}$ and T_{amb} are the temperature of the outer shell and the ambient, respectively; ε_1 and ε_g are the outer shell emissivity (0.9) and the emissivity of hot gases (0.02)²⁰, respectively; σ is the Stefan-Boltzmann constant, $F_{shell-amb}$ is the view factor between the outer shell and the ambient, and t_{exp} is the exposure duration. The $h_{conv,amb1}$ and $h_{conv,amb2}$ in equations (1) and (2) are calculated by Nusselt number (Nu)²⁷,

$$h_{conv} = Nu \frac{k_{air}(T)}{L} \quad (3)$$

where k_{air} is the thermal conductivity of the air, L is the characteristic length of outer shell. According to the empirical correlation of free convection on a vertical plate²⁷, the Nu is calculated as:

$$Nu = 0.68 + \frac{0.67Ra^{1/4}}{(1 + [0.492/Pr]^{9/16})^{4/9}} \quad 10^{-1} < Ra < 10^9 \quad (4)$$

$$Nu = 0.825 + \frac{0.387Ra^{1/6}}{(1 + [0.492/Pr]^{9/16})^{8/27}} \quad Ra > 10^9 \quad (5)$$

$$Ra = \frac{g\beta(T_{shell} - T_{amb})L^3}{\alpha\nu} \quad (6)$$

When the thermal energy is transmitted to the clothing layer, a portion of thermal energy is stored in the clothing system. The energy conservation equation of each clothing layer is given as below²⁰.

$$(\rho C_p)_{fab} \frac{\partial T}{\partial t} = \frac{\partial}{\partial x} \left(k_{fab}(T) \frac{\partial T}{\partial x} \right) - \frac{\partial q_{rad-absorb}}{\partial x} \quad (7)$$

where ρ_{fab} , $(C_p)_{fab}$ and k_{fab} are density of each fabric layer, specific heat and thermal conductivity, respectively; $q_{rad-absorb}$ is the absorbed portion of the radiant heat flux from the heat source to the outer shell. Beer’s law is employed to account for the absorption of the incident thermal radiation ($q_{rad-absorb}$) as it penetrates the pores of the fabric, i.e.²⁰,

$$q_{rad-absorb} = q_{rad} \exp(-\kappa_{fab}x) \quad (8)$$

where κ_{fab} is the extinction coefficient of the outer shell that is given by²⁷

$$\kappa_{fab} = \ln\left(\frac{1-r}{\tau}\right)/L_{fab} \quad (9)$$

where τ is the transmissivity of outer shell and L_{fab} is the thickness of outer shell. The q_{rad} in equation (8) is the incident portion of the radiant heat flux from the heating source to the outer shell, which can be expressed as,

$$q_{rad} = \frac{F_{hs-shell}\sigma(\varepsilon_{hs}T_{hs}^4 - \varepsilon_{shell}T_{shell}^4)A_{hs}}{A_{fab}} - \sigma\varepsilon_{shell}F_{shell-amb}(1 - \varepsilon_g)(T_{shell}^4 - T_{amb}^4) \quad (10)$$

where A_{hs} and A_{fab} are the heating source area and the outer shell area, respectively; T_{hs} and ε_{hs} are the temperature of heating source and the emissivity of heating source, respectively; $F_{hs-shell}$ is the fraction of the radiation leaving the heating source that strikes the outer shell.

The thermal conductivity of fabric is determined from the ratio of fiber to air fraction in the fabric as follows²⁰.

$$k_{fab}(T) = 0.8k_{air}(T) + 0.2k_{fiber}(T) \quad (11)$$

where k_{fiber} and k_{air} are the thermal conductivity of fiber and the thermal conductivity of air contained in the fabric's pores, respectively, which are individually defined as follows²⁰.

$$k_{fiber}(T) = 0.13 + 0.0018(T - 300) \quad (12)$$

$$k_{air}(T) = 0.026 + 0.000068(T - 300) \quad (13)$$

Heat transfer in the air gap between clothing and human body. The heat transfer in the air gap plays an important role in thermal insulation of protective clothing, which is determined by the coupled heat transfer of convection, conduction and radiation. This model deals with the air gap as a radiation participating medium that only absorbs thermal radiation and does not emit thermal radiation. The heat transfer model within the air gap is written as follows²⁸

$$(\rho C_p)_{air} \frac{\partial T}{\partial t} = \frac{\partial}{\partial x} \left(k_{air}(T) \frac{\partial T}{\partial x} \right) + \frac{\partial}{\partial x} q_{rad-absorb} \quad (14)$$

Where ρ_{air} and $(C_p)_{air}$ are the density and specific heat of air, respectively; and $q_{rad-absorb}$ is the absorbed portion of the radiant heat flux from the thermal to the sensor. Beer's law is employed to account for the absorption of the incident thermal radiation ($q_{therm-sen}$), i.e.,

$$q_{rad-absorb} = q_{therm-sen} (1 - \exp(-\kappa_{air}x)) \quad (15)$$

where κ_{air} is the extinction coefficient of the air gap (5 m^{-1})²⁸. The occurrence of convective heat transfer can be judged by calculating Rayleigh number (Ra), as shown in Equation (29). When the Ra is more than 1000, the natural convection in a vertical air gap is considered. The convective heat transfer in the air gap can be simulated in boundary conditions, which are written as,

$$-k_{therm} \frac{\partial T}{\partial x} \Big|_{x=L_{fab}} = q_{therm-skin} + h_{conv-air}(T_{therm} - T_{skin}) \quad (16)$$

$$-k_{ep} \frac{\partial T}{\partial x} \Big|_{x=L_{fab}+L_{air}} = q_{therm-skin} \exp(\kappa_{air}L_{air}) + h_{conv-air}(T_{therm} - T_{skin}) \quad (17)$$

where $h_{conv/cond}$ is the convective or conductive heat transfer coefficient in the air gap, which can be obtained by the equation (3). The air gap between thermal liner and skin surface can be treated as a rectangular enclosure. The Nu can be calculated by^{29,30},

$$Nu = \begin{cases} 1.0, & Ra \leq 10^3 \\ 0.22 \left(\frac{Pr}{0.2 + Pr} \right)^{0.28} \left(\frac{H}{L_{air}} \right)^{-0.25}, & 10^3 \leq Ra \leq 10^{10} \end{cases} \quad (18)$$

Human heat transfer and thermoregulation. Human body has a self-regulation function that can responds to varied thermal environments³¹. A multi-node thermal model is used to simulate human physiological responses under transient conditions with the input of human, clothing and environment parameters, such as activity intensity, clothing properties, ambient temperature, mean radiant temperature, relative humidity, and air velocity. The thermal regulation system consists of a controlling active system and a controlled passive system.

Passive system. The passive system simulates the heat transfer within body tissue layers, and between human body and the heat exposure environment through conduction, convection, radiation, and evaporation³². The proposed thermoregulatory model²⁶ divides the human body into 20 segments as that of the thermal manikin, including face, head, upper arms, forearms, hands, chest, shoulder, stomach, back, hips, thighs, calves, and feet. Each body segment has four layers: core, muscle, fat, and skin. In addition, the central blood compartment represented the blood circulation, making a total of 81-nodes²⁶. Therefore, the proposed thermoregulatory model was also called 81-node model. The heat balance of each node (core, muscle, fat, and skin), except the central blood compartment, can be described by the following equations³³:

$$c_{i,1} \frac{dT_{i,1}}{dt} = Q_{i,1} - B_{i,1} - D_{i,1} - Re s_{i,1} \quad (19)$$

$$c_{i,2} \frac{dT_{i,2}}{dt} = Q_{i,2} - B_{i,2} + D_{i,1} - D_{i,2} \quad (20)$$

$$c_{i,3} \frac{dT_{i,3}}{dt} = Q_{i,3} - B_{i,3} + D_{i,2} - D_{i,3} \quad (21)$$

$$c_{i,4} \frac{dT_{i,4}}{dt} = Q_{i,4} - B_{i,4} + D_{i,3} - (R_{i,4} + C_{i,4} + E_{i,4}) \quad (22)$$

where i (from 1 to 20) refers to the body segments; j (1, 2, 3, 4) refers to the four layers of core, muscle, fat, and skin, respectively; The left terms in Eqs 19~22 are the rate of heat storage of core, muscle, fat, and skin, respectively; c_{ij} is the heat capacity; T_{ij} is the body temperature; Q_{ij} is the rate of heat production; B_{ij} is the heat exchange between each node and the central blood node; D_{ij} is the heat exchange by conduction to the neighbor layer within the segment; Res_{ij} is the heat loss by respiration; and $C_{i,4}$, $R_{i,4}$ and $E_{i,4}$ are the heat loss through convection, radiation, and evaporation from skin, respectively.

The heat balance of the central blood compartment is calculated as follows²⁶:

$$c_{81} \frac{dT_{81}}{dt} = \sum_{i=1}^{20} \sum_{j=1}^4 B_{i,j} \quad (23)$$

where, the left term in Eq. 23 is the heat storage rate of the central blood compartment; the right term in Eq. 23 is the total heat exchange between each node and the central blood node through convection; c_{81} and T_{81} are the heat capacity and the temperature of the central blood compartment, respectively.

Active system. The active system simulates vasodilatation, vasoconstriction, sweating, and shivering using warm and cold signals, which are received by the warm and cold receptors, respectively³³. Those signals are calculated by the temperature difference between each node and its set point ($Err = T - T_{set}$). If $Err > 0$ (vasodilatation and sweating occur), then $Wrm = Err$, $Cld = 0$. If $Err < 0$ (vasoconstriction and shivering occur), then $Cld = -Err$, $Wrm = 0$. Here Wrm and Cld are the warm and cold signals, respectively. The weighted warm skin signals ($Wrms$) and cold skin signals ($Clds$) are used as the control variables to regulate physiological reaction. The control equations for vasodilatation, vasoconstriction, sweating and shivering are expressed as follows, respectively:

$$D_L = C_{dl}Err(1) + S_{dl}(Wrms - Clds) + P_{dl}Wrm(1)Wrms \quad (24)$$

$$S_T = -C_{st}Err(1) - S_{st}(Wrms - Clds) + P_{st}Cld(1)Clds \quad (25)$$

$$S_w = C_{sw}Err(1) + S_{sw}(Wrms - Clds) + P_{sw}Wrm(1)Wrms \quad (26)$$

$$C_h = -C_{ch}Err(1) - S_{ch}(Wrms - Clds) + P_{ch}Cld(1)Clds \quad (27)$$

where D_L , S_T , S_w , and C_h are the signals for vasodilatation, vasoconstriction, sweating, and shivering, respectively. C_{dl} , S_{dl} , P_{dl} , C_{st} , C_{st} , S_{st} , P_{st} , C_{sw} , S_{sw} , P_{sw} , C_{ch} , S_{ch} , and P_{ch} are the control coefficients. Based on the work of Stowijk³³ and Tanabe *et al.*³⁴, these control coefficients are modified according to the surface area and weight of each body segment. $Err(1)$, $Wrm(1)$, and $Cld(1)$ are the error signal, warm signal, and cold signal of core layer.

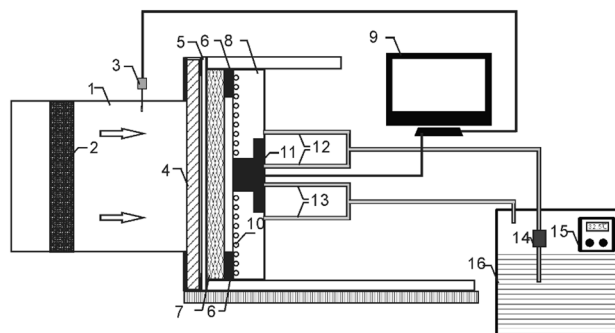
Numerical computation. The developed model is composed of transient partial differential and ordinary differential equations. A finite difference scheme is applied to obtain the numerical solution. The Crank-Nicholson implicit scheme is applied to discretize the transient partial differential equations based on a (non-uniform) grid spanning a 1D space coordinate and time coordinate. A non-linear tri-diagonal system is obtained by discretizing the boundary conditions. Due to nonlinearity that comes from the radiation boundary condition, the coupling conduction-radiation, and the variation in the fabric thermo-physical and convective heat transfer coefficient with temperature, the Gauss-Seidel point-by-point iterative scheme is employed to solve these discrete equations. The central difference method is applied to calculate the ordinary differential equation. Specifically, the model parameters and temperatures from the previous time step are used as initial values for the iteration loop. The space-step and time-step are defined as 5×10^{-6} m and 0.1 s, respectively.

Layer	Component	Thickness (mm)	Density (kg/m ³)	Specific heat (J/(kg K))	Thermal conductivity (W/(m K))
Outer shell	100% Nomex	0.6	342	1570	0.047
Moisture barrier	80% Nomex/20% Kevlar (PTFE)	0.9	122	1160	0.034
Thermal liner	100% M-aramid	2.2	123	1350	0.035

Table 1. Properties of the fabrics used in the numerical simulation.

Parameter	Symbol	Unit	Value
Heating source temperature	T_{hs}	K	733.15
Hot gases	ϵ_g	—	0.02
Heating source area	A_{hs}	m ²	0.0144
Sensor area	A_{sen}	m ²	0.01
Heat source emissivity	ϵ_{hs}	—	0.98
Sensor emissivity	ϵ_{sen}	—	0.90

Table 2. Basic parameters of the heating source and the sensor.



1. heat exposure box; 2. heating source; 3. temperature sensor; 4. insulation board; 5. specimen holder; 6. spacer block; 7. specimen; 8. data collection sensor; 9. data acquisition system; 10. copper tubes; 11. data collection; 12. water inlet; 13. water outlet; 14. pump; 15. temperature control; 16. water tank

Figure 2. Diagram of heat transfer tester for low-level radiation³⁵.

Experimental test

Materials. Flame-resistant fabrics widely used in the firefighting protective clothing were selected to validate the developed model. The basic properties of the selected fabrics were shown in Table 1. The thickness of test specimens was measured in accordance with standard ASTM D 1777–96. The mass per unit area was tested based on an electronic scale tester, conformed with standard ASTM D3776–96. The laser pulse method and differential scanning calorimeter (NETZSCH DSC 204 F1) tests were employed to measure thermal conductivity and specific heat of the fabrics.

Methods. A bench top tester that measures skin heat flux in radiant heat exposure was used to validate the developed model, as shown in Fig. 2³⁵. The radiant heat flux ranged from 0 to 21 kW/m² can be produced by a black ceramic heat source. The skin heat flux was measured by a water cooled Schmidt-Boelter thermopile type sensor (Medtherm Corporation, USA). According to ASTM F2731–11, the parameters of heat source and skin-simulant sensor are given in Table 2. A 6.4 mm air gap between the clothing and the sensor assembly was simulated by inserting a 6.4 mm spacer.

The fabric samples were conditioned in a constant temperature and humidity chamber (25 °C and 65% relative humidity) for at least 24 hours. The testing apparatus was firstly calibrated, and then the fabric system was modeled in a vertical orientation, subjected to a radiant heat source with a nominal heat flux of 8.5 kW/m² for 300 s. The ambient temperature and relative humidity were approximately 30 °C and 65%, respectively. After the heat exposure, the skin-simulant sensor continued to record the skin heat flux for 300 s, as cooling phase. The obtained skin heat flux was treated as the boundary condition of human thermo-regulation model to calculate mean skin and core temperatures. Each specimen was tested three times and the average value was obtained.

Results and Discussion

Model verification. Core temperature and mean skin temperature are two of the most important human physiological responses. The proposed model was applied to predict the core temperature and mean skin

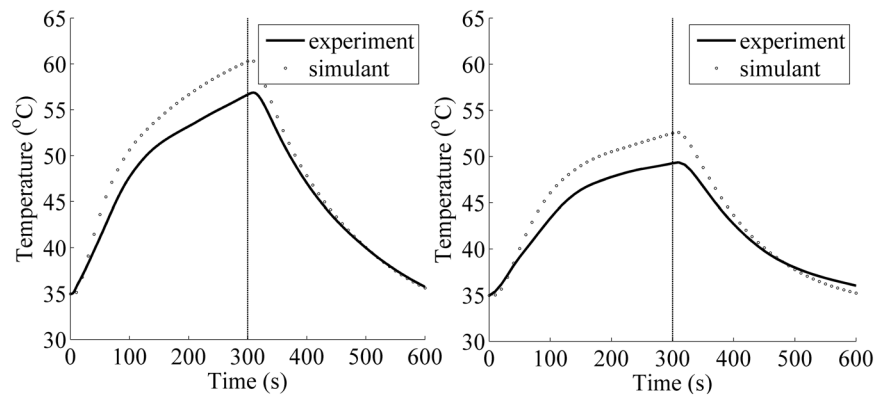


Figure 3. Comparison of mean skin temperature between the experiment and the simulant results: (a) without an air gap; (b) with an air gap.

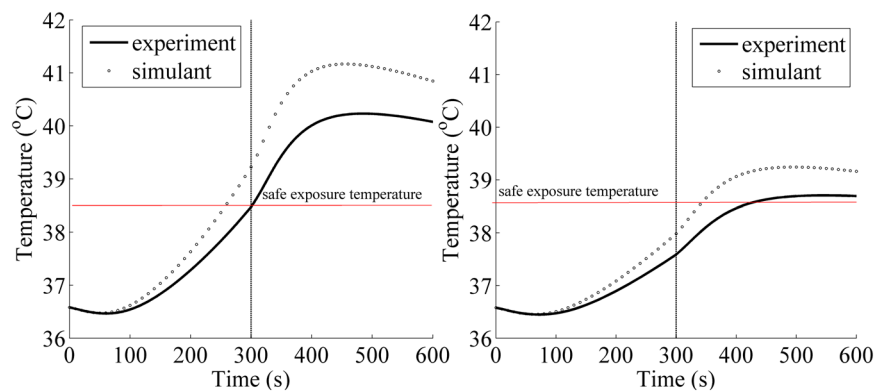


Figure 4. Comparison of the core temperature between the experiment and the simulated results: (a) without an air gap; (b) with an air gap.

temperature of firefighter in a typical firefighting environment with a metabolic rate of 290 W/m^2 ³⁶. The predicted mean skin temperatures were compared with those from the experimental test, as shown in Fig. 3. The overall trend of simulant and experiment results presented a good agreement, indicating that the developed model could predict thermal response of human body in low level thermal radiation. In heat exposure of 300 seconds, the increasing rate of the mean skin temperature predicted by the model was larger than that from the experiment. The maximum predicted deviation for two cases (without and with air gap) were 3.63 and 3.26 °C, respectively. The difference could be attributed to ignorance of the multi-dimensional heat transfer and the coupled heat and moisture transfer in the clothing. It was reported that the central temperature for the heated region of protective fabric was higher than the surrounding temperatures, thus the thermal energy from the central zone of protective fabric could be transferred to the surrounding zone³⁷. The moisture transfer in protective fabric presented a complex impact on the heat transfer in different heat exposure conditions³⁸. However, a positive effect of moisture transfer was found in low intensity radiant exposure due to the heat storage and the evaporative heat loss of moisture²⁵, which could decrease the temperature rise of skin. After the heat exposure of 300 seconds, the temperature difference between the model prediction and the experiment gradually decreased. This was due to the fact that the temperature difference between human skin and ambience determines the cooling rate of human body. Additionally, the moisture within the protective fabric increased the fabric's heat capacity²⁵. As a result, more stored thermal energy was discharged and reducing the cooling rate after the exposure.

Figure 4(a,b) show comparison of the core temperature prediction with the experiments in protective clothing without and with an air gap, respectively. A larger increase rate of the core temperature was observed for the model prediction. The core temperature continued to increase after the heat exposure of 300 seconds because of a lag effect of heat transfer from the clothing to human body. The differences of the core temperature between the model prediction and the experiment without and with an air gap were 0.75 and 0.40 °C, respectively. The core temperature normally maintains within 37.0 ± 1.0 °C³⁹. The core temperature of less than 38.5 °C could be defined as safe exposure temperature^{40,41}, and the corresponding time for the core temperature to stay at less than 38.5 °C was treated as safe exposure time. It was clear that the safe exposure time from the experiment without and with an air gap were 301.6 and 407.0 seconds, which presented a difference of 14.5% and 17.1% compared with the simulant results, respectively. For the clothing system without air gap, the difference of the safe exposure time was resulted from the core temperature difference during heat exposure. However, the core temperature difference during cooling phase increased the difference of the safe exposure time for the clothing system with an air gap.

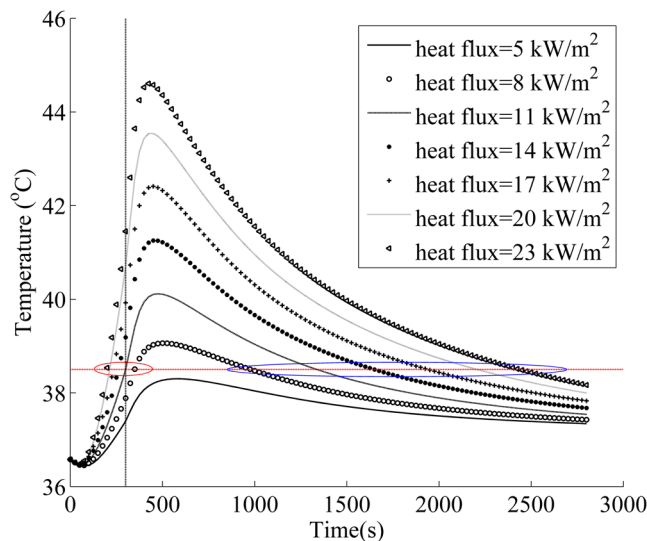


Figure 5. Change of core temperature over time in radiant heat exposure of 5 to 23 kW/m². (Note: the red line indicates the limit value of human physiological strain^{40,41}; the intersections in red wireframe indicate the safe exposure time; the intersections in blue wireframe indicate the effective cooling time).

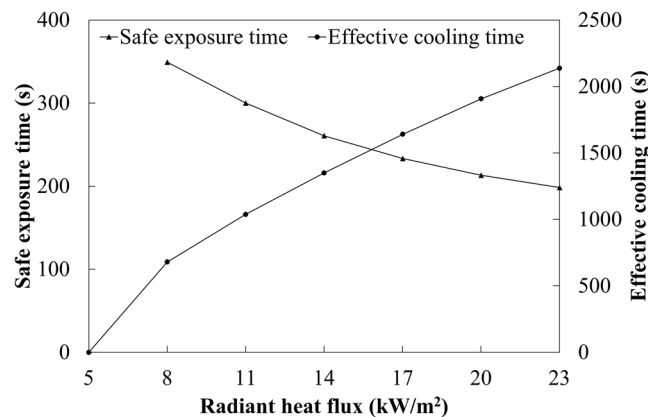


Figure 6. Change of safe exposure time and effective cooling time with radiant heat flux.

Effect of radiant intensity. Firefighters in fire-fighting and emergency rescue are usually exposed to low-level thermal radiation that ranges from 2.1 to 21 kW/m²⁶. In order to obtain the safe exposure time of firefighter in different intensity of heat exposure, the proposed model was used to predict core temperature in radiant heat exposure of 5 to 23 kW/m², as shown in Fig. 5. The exposure and cooling times in the simulation were 300 and 2500 seconds, respectively. It was found that the rise of radiant exposure intensity increased the core temperature of human body. The highest core temperature did not occur in the heat exposure phase, but in the cooling phase. This was because the discharge of stored thermal energy in the clothing layer and the delay effect of heat transfer continued to increase the core temperature²². After around 500 seconds, the core temperature began to decrease due to the heat loss to the cooling environment. In the cooling phase, the core temperature showed an increase with the rising of radiant heat flux, while the difference of core temperature between different heat fluxes reduced over time.

According to the above discussion, firefighter could be subjected to heat stress when the core temperature is above 38.5 °C. The time range in which the core temperature reaches above 38.5 °C is defined as dangerous time zone of firefighter^{40,41}. The dangerous time zone in different heat exposures can be found in Fig. 5. The dangerous time zones start from the safe exposure time and end by the effective cooling time. Figure 6 illustrates the variation of safe exposure time and effective cooling time against radiant heat flux. The core temperature for the radiant heat flux of 5 kW/m² was found to be less than 38.5 °C during the heat exposure and cooling phases. This indicated that the protective clothing could provide effective thermal protection for firefighter in radiant heat flux of 5 kW/m². The increased radiant heat flux reduced the safe exposure time and increased the effective cooling time. But the change rates of safe exposure time was relatively less than that of effective cooling time. This indicated that the radiant heat flux had greater influence on the effective cooling time. The result illustrated that the cooling effect in rest environment of 30 °C could not instantly take firefighters out of danger. For radiant heat flux of 23 kW/m², firefighter would need at least 2136 seconds to recover to normal state after the heat exposure of 300 seconds.

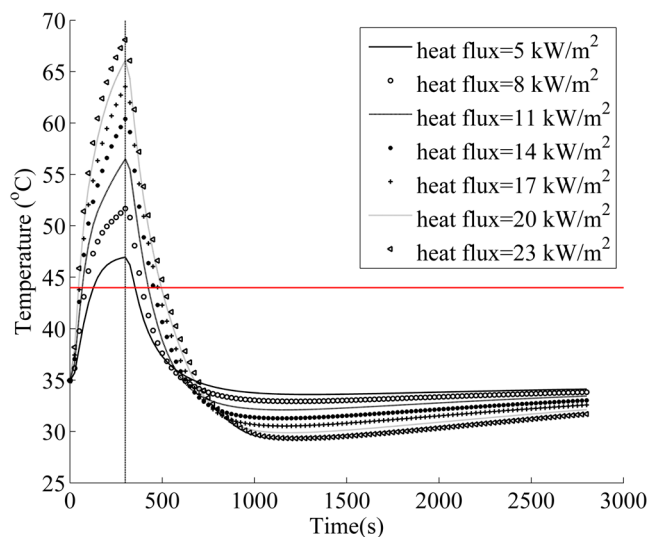


Figure 7. Change of mean skin temperature with time in radiant heat exposure of 5 to 23 kW/m². (Note: the red line indicates the threshold value of skin burn)⁴³.

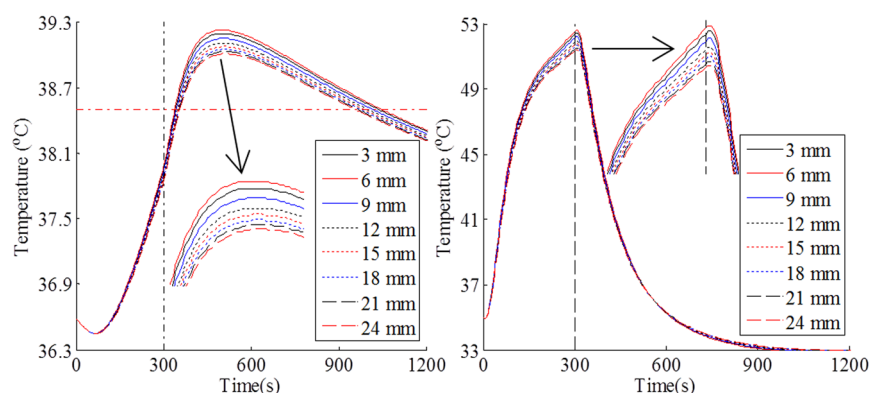


Figure 8. Changes of core temperature (a) and mean skin temperature (b) with time in an air gap of 0 to 24 mm. (Note: the red dot dash line indicates the limit value of human physiological strain)^{40,41}.

Figure 7 shows the effect of radiant heat flux on the mean skin temperature of firefighter wearing a clothing system with an air gap. The difference of the mean skin temperature between different radiative heat fluxes gradually reduced with the increase of radiant heat flux. After heat exposure, the mean skin temperature reduced rapidly especially for the higher heat flux. Thus, the change of the mean skin temperature presented an obviously different behavior from the change of core temperature. The mean skin temperature was less than 44 °C after 500 seconds, indicating that the skin layer did not continue to produce burn since 44 °C is a threshold value of skin burn⁴². These results revealed that the physiological heat strain of human body lasted for longer time than skin burn in radiant heat exposure.

Effect of air gap size. Due to the much lower thermal conductivity, air gap between the clothing and the human body can provide high thermal insulation against fire hazards. However, the thermal insulation effect could be overshadowed by the natural heat convection effect with an increase of the size of the air gap. It was reported that the average air gap size between the clothing and the body is around 25 mm⁹. Therefore, the air gap ranging from 0 to 24 mm was used in the developed model for investigating the relationship between the air gap size and the physiological strain of human body. Figure 8(a,b) show the effect of air gap size on core temperature and mean skin temperature predicted by numerical model, respectively. Figure 8 does not present the temperature changes for 0 mm air gap since the core and mean skin temperatures for 0 mm air gap were obviously higher than that for other air gaps. This indicated that the existence of an air gap of small size had a significant effect on preventing heat strain. Therefore,

When the air gap size was increased from 3 to 24 mm, the core temperature and mean skin temperature increased firstly and then decreased. For clothing with a 6 mm air gap, the peak values for both core temperature and mean skin temperature were the largest among all air gaps. The increased air gap size, while reducing the thermal conductivity, could also increase the convective heat transfer rate from the inner side of clothing to the human body. The natural convection in air gaps depends not only on the size and orientation of the air gap,

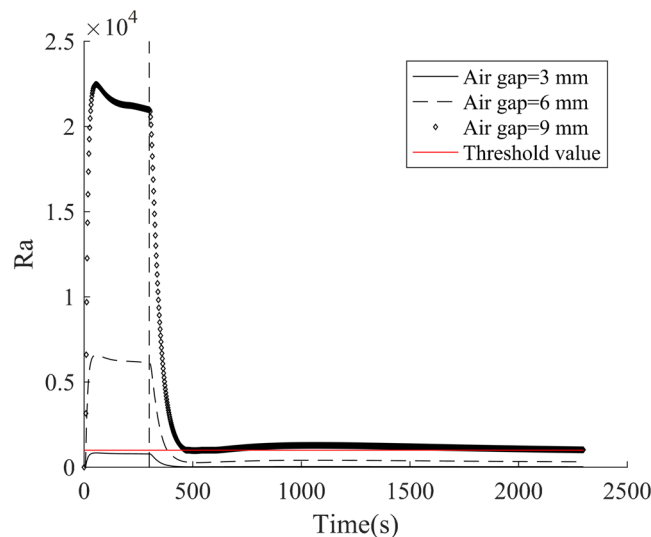


Figure 9. Change of Ra with time in an air gap of 3 to 9 mm. (Note: the red line indicates the threshold value for the occurrence of convection heat transfer⁴⁵).

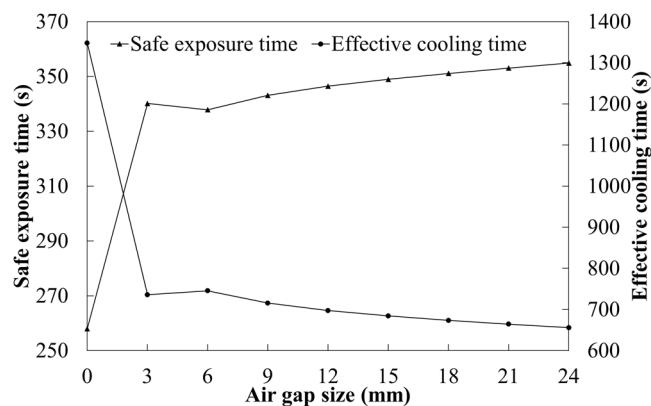


Figure 10. Change of safe exposure time and effective cooling time with air gap size.

but also on the intensity of heat exposure⁴³. Previous studies reported the occurrence of natural convection in a horizontal air gap with a size of 6–7 mm⁴⁴. The corresponding Rayleigh number (Ra) in the air gap was more than 1708⁴⁵. For the vertical air gap, however, the convective heat transfer occurred when Ra was more than 1000⁴⁵. Figure 9 shows the change of Ra in a vertical air gap with time. It was clear that Ra increased greatly with the increase of the size of air gap. The convective heat transfer during heat exposure initiated in an air gap that is more than 3 mm. It could continue to exist in the air gaps of larger than 9 mm in the cooling phase. In addition, the air gap size had an important effect on the cooling effect of human body. The air gap resisted heat loss from the human body to the surrounding environment. When there is no air gap, the core temperature and mean skin temperature presented the rapidest decrease during the cooling. The temperature difference between the different air gap sizes gradually decreased with cooling time.

As can be seen from Fig. 8(a), the core temperatures of different air gap sizes were higher than the limit value of human physiological strain. According to the intersection of core temperature and safe exposure temperature, the safe exposure time and the effective cooling time over air gap size are obtained and showed in Fig. 10. As the air gap size increased, the safe exposure time showed an increase, while the effective cooling time obviously decreased. The safe exposure time of air gap of 24 mm was 1.38 times that of no air gap. The effective cooling time of no air gap was more than twice that of air gap of 24 mm. This indicated that the increase of air gap size could reduce the dangerous time zone of core temperature. However, when the air gap size was larger than 6 mm, the safe exposure time and effective cooling time presented an opposite tendency against the air gap size. As discussed above (see Fig. 9), the convective heat transfer occurred in an air gap of 6 mm, which could enhance heat transfer between protective clothing and human body. Although the convective heat transfer rate gradually increased with the air gap size, the radiative and conductive heat transfer showed a decrease⁴⁵. Therefore, the safe exposure time continued to increase with the increase of the air gap size when the size exceeded 6 mm.

Conclusions

A numerical model that consists of both heat transfer in firefighting protective clothing and human thermal regulation was developed to predict physiological heat strain of firefighter in low-level thermal radiation. The model was validated from the experiment simulation. Based on the parameter study of the model, it was found that the intensity of radiative heat exposure was an important factor influencing the human physiological strain. The increase of its intensity linearly shortened the safe exposure time and increased the effective cooling time. When the air gap size was smaller than 6 mm, the human physiological strain was reduced by the increased air gap size. However, the occurrence of convective heat transfer increased the total heat transfer from the clothing to the human body when the air gap size was equal or exceeding 6 mm. Thus, the developed model is capable of simulating heat transfer in multi-layered protective clothing with an air gap. It can be used to effectively predict the thermal response of firefighter in fire hazards. The findings in this study provide a fundamental understanding of material engineering and safe operation, and proper training of firefighter in fire hazards.

References

- Fahy, R., LeBlanc, P. & Molis, J. Firefighter Fatalities in the United States: 2014. National Fire Protection Association. (2016).
- Kim, J. H., Williams, W. J., Coca, A. & Yokota, M. Application of thermoregulatory modeling to predict core and skin temperatures in firefighters. *International Journal of Industrial Ergonomics* **43**, 115–120 (2013).
- Von Heimburg, E. D., Rasmussen, A. K. R. & Medbo, J. I. Physiological responses of firefighters and performance predictors during a simulated rescue of hospital patients. *Ergonomics* **49**, 111–126 (2006).
- ASTM F2703-13 Standard test method for unsteady-state heat transfer evaluation of flame resistant materials for clothing with burn injury prediction. (American Society for Testing and Materials, 2013).
- ASTM F2702-15, Standard test method for radiant heat performance of flame resistant clothing materials with burn injury prediction. (American Society for Testing and Materials, 2013).
- ASTM F2731-11, Standard test method for measuring the transmitted and stored energy of firefighter protective clothing systems. (American Society for Testing and Materials, 2011).
- Young Moo, L. & Barker, R. L. Thermal protective performance of heat-resistant fabrics in various high intensity heat exposures. *Textile Research Journal* **57**, 123–132 (1987).
- Hummel, A., Barker, R. L., Lyons, K., Deaton, A. S. & Morton-Aslanis, J. Development of instrumented manikin hands for characterizing the thermal protective performance of gloves in flash fire exposures. *Fire Technology* **47**, 615–629 (2010).
- Song, G. Clothing air gap layers and thermal protective performance in single layer garment. *Journal of industrial textiles* **36**, 193–205 (2007).
- Mah, T. & Song, G. Investigation of the contribution of garment design to thermal protection. Part 1: characterizing air gaps using three-dimensional body scanning for women's protective clothing. *Textile Research Journal* **80**, 1317–1329 (2010).
- Torvi, D. A. & Hadjisophocleous, G. V. Research in protective clothing for firefighters: State of the art and future directions. *Fire Technology* **35**, 111–130 (1999).
- Crown, E. M., Ackerman, M. Y., Dale, J. D. & Tan, Yb Design and evaluation of thermal protective flightsuits. part ii: instrumented mannequin evaluation. *Clothing and Textiles Research Journal* **16**, 79–87 (1998).
- Barr, D., Gregson, W. & Reilly, T. The thermal ergonomics of firefighting reviewed. *Applied ergonomics* **41**, 161–172 (2010).
- Ftaiti, F., Duflot, J. C., Nicol, C. & Grelot, L. Tympanic temperature and heart rate changes in firefighters during treadmill runs performed with different fireproof jackets. *Ergonomics* **44**, 502–512 (2001).
- Lee, J. Y., Kim, S., Jang, Y. J., Baek, Y. J. & Park, J. Component contribution of personal protective equipment to the alleviation of physiological strain in firefighters during work and recovery. *Ergonomics* **57**, 1068–1077 (2014).
- Hemmatjo, R., Motamedzade, M., Aliabadi, M., Kalatpour, O. & Farhadian, M. The Effect of Various Hot Environments on Physiological Responses and Information Processing Performance Following Firefighting Activities in a Smoke-Diving Room. *Safety and Health at Work* (2017).
- Annaheim, S. *et al.* Internal and external heat load with fire fighter protective clothing: data from the lab and the field. Paper presented at 16th *International Conference on Environmental Ergonomics (ICEE)*, Portsmouth, United Kingdom. University of Portsmouth. (2015 June 28–July 3).
- Fontana, P. *et al.* Thermo-physiological impact of different firefighting protective clothing ensembles in a hot environment. *Textile Research Journal*, 0040517516688629 (2017).
- Morse, H. L., Thompson, J. G., Clark, K. J., Green, K. A. & Moyer, C. B. Analysis of the thermal response of protective fabrics. (DTIC Document, 1973).
- Torvi, D. A. *Heat Transfer In Thin Fibrous Materials Under High Heat Flux Conditions* PHD thesis, University of Alberta, (1997).
- Song, G. W. *et al.* Modeling the thermal protective performance of heat resistant garments in flash fire exposures. *Textile Research Journal* **74**, 1033–1040 (2004).
- Su, Y., He, J. & Li, J. Modeling the transmitted and stored energy in multilayer protective clothing under low-level radiant exposure. *Applied Thermal Engineering* **93**, 1295–1303 (2016).
- Pennes, H. H. Analysis of tissue and arterial blood temperatures in the resting human forearm. *Journal of applied physiology* **1**, 93–122 (1948).
- Abbott, N. J. & Schulman, S. Protection from fire: Nonflammable clothing — A review. *Fire Technology* **12**, 204–218 (1976).
- Prasad, K., Twilley, W. H. & Lawson, J. R. *Thermal performance of fire fighters' protective clothing: numerical study of transient heat and water vapor transfer*. (US Department of Commerce, Technology Administration, National Institute of Standards and Technology, 2002).
- Yang, J., Weng, W. & Zhang, B. Experimental and numerical study of physiological responses in hot environments. *Journal of Thermal Biology* **45**, 54–61 (2014).
- Bergman, T. L. & Incropera, F. P. *Fundamentals of heat and mass transfer* (eds Bergman, T. L. & Incropera, F. P.), 434–655 (Wiley, 2011).
- Ghazy, A. & Bergstrom, D. J. Numerical simulation of transient heat transfer in a protective clothing system during a flash fire exposure. *Numerical Heat Transfer, Part A: Applications* **58**, 702–724 (2010).
- Hollands, K., Raithby, G. D. & Konicek, L. Correlation equations for free convection heat transfer in horizontal layers of air and water. *International Journal of Heat and Mass Transfer* **18**, 879–884 (1975).
- Ostrach, S. Natural convection in enclosures. *Journal of Heat Transfer* **110**, 1175–1190 (1988).
- Hensley, D. W. *et al.* 50 Years of Computer Simulation of the Human Thermoregulatory System. *Journal of biomechanical engineering* **135**, 1–9 (2013).
- Fiala, D., Havenith, G., Bröde, P., Kampmann, B. & Jendritzky, G. UTCI-Fiala multi-node model of human heat transfer and temperature regulation. *International journal of biometeorology* **56**, 429–441 (2012).
- Stolwijk, J. A. Mathematical models of thermal regulation. *Annals of the New York Academy of Sciences* **335**, 98–106 (1980).

34. Tanabe, Si, Kobayashi, K., Nakano, J., Ozeki, Y. & Konishi, M. Evaluation of thermal comfort using combined multi-node thermoregulation (65MN) and radiation models and computational fluid dynamics (CFD). *Energy and Buildings* **34**, 637–646 (2002).
35. Su, Y. & Li, J. *Development of a test device to characterize thermal protective performance of fabrics against hot steam and thermal radiation. Measurement Science & Technology* **27**, 1–12 (2016).
36. ISO 8996 Ergonomics of the thermal environment—determination of metabolic rate. (International Organization for Standardization, 2004).
37. Sawcyn, C. M. J. & Torvi, D. A. Improving heat transfer models of air gaps in bench top tests of thermal protective fabrics. *Textile Research Journal* **79**, 632–644 (2009).
38. Lawson, L. K., Crown, E. M., Ackerman, M. Y. & Dale, J. D. Moisture effects in heat transfer through clothing systems for wildland firefighters. *International journal of occupational safety and ergonomics* **10**, 227–238 (2004).
39. Wissler, E. H. Whole-body human thermal modeling, an alternative to immersion in cold water and other unpleasant endeavors. *Journal of Heat Transfer* **134**, 031019 (2012).
40. Yang, Y. & Chan, A. P. Perceptual strain index for heat strain assessment in an experimental study: an application to construction workers. *Journal of thermal biology* **48**, 21–27 (2015).
41. McLellan, T. M. The importance of aerobic fitness in determining tolerance to uncompensable heat stress. *Comparative Biochemistry and Physiology Part A: Molecular & Integrative Physiology* **128**, 691–700 (2001).
42. Henriques, F. C. Studies of thermal injury; the predictability and the significance of thermally induced rate processes leading to irreversible epidermal injury. *Archives of pathology* **43**, 489–502 (1947).
43. Talukdar, P., Das, A. & Alagirusamy, R. Numerical modeling of heat transfer and fluid motion in air gap between clothing and human body: Effect of air gap orientation and body movement. *International Journal of Heat and Mass Transfer* **108**, 271–291 (2017).
44. Torvi, D. A. & Dale, J. D. Heat transfer in thin fibrous materials under high heat flux. *Fire technology* **35**, 210–231 (1999).
45. Cengel, Y. A., Ghajar, A. J. & Ma, H. *Heat and Mass Transfer: Fundamentals & Applications* (eds Cengel, Y. A., Ghajar, A. J. & Ma, H.), (McGraw-Hill, 2011).

Acknowledgements

The authors would like to acknowledge the financial support from the National Nature Science Foundation (Grant NO. 51576038), Donghua University PhD Thesis Innovation Funding (Grant NO. 16D310701), and Shanghai Municipal Natural Science Foundation (Grant NO. 17ZR1400500).

Author Contributions

Yun Su, Jie Yang and Guowen Song conceived and designed the scheme and wrote the manuscript. Yun Su and Jie Yang conducted the analysis of numerical simulation. Rui Li and Chunhui Xiang provided suggestions for the paper. The experimental section in this paper was performed under the instruction of Jun Li. All authors reviewed the manuscript.

Additional Information

Competing Interests: The authors declare no competing interests.

Publisher's note: Springer Nature remains neutral with regard to jurisdictional claims in published maps and institutional affiliations.



Open Access This article is licensed under a Creative Commons Attribution 4.0 International License, which permits use, sharing, adaptation, distribution and reproduction in any medium or format, as long as you give appropriate credit to the original author(s) and the source, provide a link to the Creative Commons license, and indicate if changes were made. The images or other third party material in this article are included in the article's Creative Commons license, unless indicated otherwise in a credit line to the material. If material is not included in the article's Creative Commons license and your intended use is not permitted by statutory regulation or exceeds the permitted use, you will need to obtain permission directly from the copyright holder. To view a copy of this license, visit <http://creativecommons.org/licenses/by/4.0/>.

© The Author(s) 2018